On the Orientation of Quinoline on Pd{111}: Implications for Heterogeneous Enantioselective Hydrogenation

Jonathan M. Bonello,[†] Robert Lindsay,[‡] Ashok K. Santra,[§] and Richard M. Lambert*,[†]

Chemistry Department, Cambridge University, Cambridge CB2 1EW, England

Received: October 10, 2001; In Final Form: December 14, 2001

The adsorption geometry of quinoid species at platinum and palladium surfaces is relevant to an understanding of enantioselective catalytic hydrogenation. Accordingly, quinoline multilayers and monolayers on Pd{111} have been characterized by XPS and the adsorption geometry within the monolayer determined by NEXAFS at 295 K and 360 K. The molecule lies approximately flat ($\alpha < 18° \pm 5°$), bound to the Pd{111} surface predominantly via the aromatic π-system. This adsorption geometry remains unaffected upon heating to 360 K, and the adsorbed layer does not exhibit long range order under any conditions. Comparison with the corresponding results for Pt{111} indicates that the different intrinsic rates and the reversal in the sense of enantioselectivity observed for pyruvate hydrogenation on palladium catalysts relative to platinum is unlikely to originate in either significantly different modifier adsorption geometries or spatial distributions in the two cases. In addition, it now seems less likely that the collapse in enantioselectivity observed beyond ~320 K on quinoid-modified palladium catalysts originates in a change in the adsorption geometry of the anchoring moiety of the chiral modifier.

1. Introduction

The enantioselective hydrogenation of alkyl pyruvates to the corresponding lactates in the presence of platinum catalysts modified by the cinchona alkaloids has been the subject of detailed studies as the reaction is one of only very few effective heterogeneous enantioselective systems.[1−4] In these systems, a chiral adsorbate is used to impart chirality to an intrinsically achiral metal surface: the resulting chiral adsorption sites are believed to act as centers for the enantioselective reaction. Such reactions constitute a relatively unexplored field whose practical implications are potentially far reaching as, under appropriate conditions, they afford both a high degree of stereochemical control and large rate enhancement effects. Although the number of known systems is increasing, the subject as a whole remains at an early stage of development. This is especially true in regard to fundamental studies of the surface phenomena involved, even in the case of the most studied reactions.[1−4]

The most widely accepted reaction model for the platinum-catalyzed enantioselective hydrogenation of alkyl pyruvates—the so-called *1:1 interaction model*—is based on the hypothesis that individual modifier molecules, anchored to the metal surface via the quinoline moiety, act to generate chiral adsorption sites in their immediate vicinity without the need for ordered adsorption.[1−4] Depending on whether the platinum surface is modified by cinchonidine or cinchonine (its near enantiomer) subsequent hydrogenation of methyl pyruvate provides the (*R*)- or (*S*)-methyl lactate product, respectively, in enantiomeric excess.[1−4] Concomitant with enantioselectivity is a significant increase in rate, the enantioselective reaction being up to 50 times faster than the racemic reaction i.e., reaction in the absence of the alkaloid modifier.[1−4]

SCHEME 1

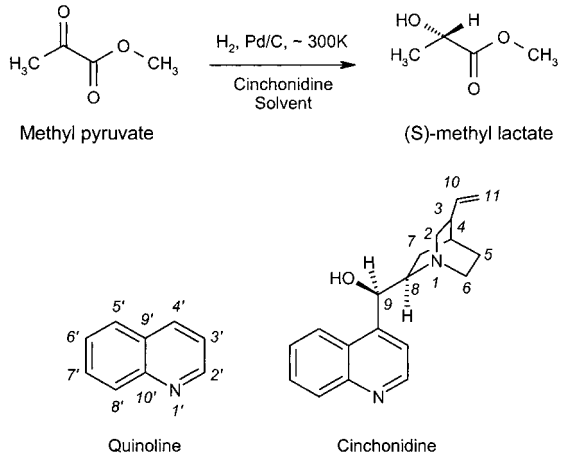

The corresponding palladium-catalyzed prototype reaction, shown in Scheme 1, has been less rigorously investigated.[3,5−7] Two distinctive features of this reaction are that (i) there is little or no rate enhancement and (ii) the sense of enantioselectivity observed is *reversed* with respect to that of the Pt system (i.e., cinchonidine directs the reaction to the (*S*)-lactate product and cinchonidine to the (*R*)-product).[5−7] Both observations suggest that there must be very significant mechanistic differences between the palladium-catalyzed enantioselective reaction and the analogous platinum-catalyzed reaction.[5−7]

Broadly speaking, there are three plausible classes of explanation for the reversal in the observed stereochemical outcome of the reaction at these two metal surfaces, involving variously the reactant, or the solvent, or the chiral modifier. Concerning the reactant, deuterium tracer studies have shown that, over Pt, there is direct addition of two deuterium atoms

* To whom correspondence should be addressed. E-mail: rml1@cam.ac.uk. Phone: +44.1223.336467. Fax: + 44.1223.336362.
[†] Chemistry Department.
[‡] Present address: Chemistry Department, Manchester University, Manchester M13 9PL England.
[§] Present address: Chemistry Department, Texas A&M University, College Station, TX 77843.

10.1021/jp013765h CCC: $22.00
Published on Web 02/13/2002

across the pyruvate C═O bond,[6] whereas over Pd the main product forming route is via the corresponding enolate tautomer, thus involving C═C hydrogenation.[6,8] More recently it has also been shown that differing solvent/substituent effects at Pt and Pd surfaces, both during the catalyst modification procedure and thereafter during the asymmetric hydrogenation reaction, can strongly influence the direction of enantioselectivity in this reaction.[7]

The third possible factor that may contribute to the observed reversal of enantioselectivity with Pd catalysts is a change in the adsorption geometry and/or spatial distribution of the chiral modifier molecule, relative to Pt. This could involve a change in the orientation and/or degree of long range order of the quinoline-anchoring moiety on palladium surfaces relative to platinum surfaces. Such an effect would be expected to have a direct impact on the ease of formation of the crucial modifier−reactant complex in the enantio-differentiation step of the reaction.[1,2] We have already carried out a detailed investigation[9] of the adsorption, reactivity and orientation of quinoline on Pt{111}, the latter results being broadly in accord with those found for the orientation of 10,11-dihydrocinchonidine (DHC)[10] on the same surface, confirming the expectation that adsorption geometry is dominated by the interaction between the quinoid "footprint: and the metal surface.

Accordingly, carbon and nitrogen K-edge NEXAFS data have now been acquired to determine the orientation of quinoline with respect to the Pd{111} surface. The system has been studied at ∼295 K (the temperature used for the enantioselective reaction) and at ∼360 K (beyond the temperature of enantioselectivity collapse[1−4]). The {111} surface of palladium was chosen because in practice it is found that the enantioselective reaction proceeds efficiently only on Pt and Pd particles whose size exceeds 3 nm[11] and whose surfaces should therefore be dominated by low index planes. The results are discussed with respect to the analogous data already acquired for quinoline/Pt{111}[9] and in regard to the mechanism of chiral induction and the possible origin of enantioselectivity collapse in the asymmetric hydrogenation of α-ketoesters on Pt catalysts.

2. Experimental Methods

The XP and NEXAFS spectra for quinoline on Pd{111} were obtained on beamline 1.1 at the Daresbury SRS. Surface concentrations of the adsorbed species and their stoichiometric ratios were derived from the corresponding XP spectra using standard analysis methods.[12] NEXAFS[13] spectra at the C and N K-edges were acquired in partial electron yield (PEY) mode at several angles between normal ($\theta = 90°$) and grazing incidence ($\theta = 20°$), and were used to quantify the orientation of the adsorbate with respect to the single-crystal surface plane. The PEY detector consisted of two high transmission metal grids and a dual channel plate array. While the first grid was maintained at ground potential, retarding voltages of −200 and −320 V were applied to the second grid for the carbon and nitrogen K-edge spectra, respectively. The absolute energy scale calibration of the monochromator was found to be consistent to ±0.5 eV. The photon energy resolution at both the carbon and nitrogen K-edges was ∼0.5 eV. Repeated experimental measurements of the same system showed that the error in the final value of the molecular tilt angle, α, was of the order of ±5°. LEED observations were made with a conventional three-grid system.

To remove air and other volatile impurities, quinoline (Fluka, purum. >97%) was subjected to several freeze−pump−thaw cycles and subsequently freshly distilled under vacuum prior to all experiments. The molecule was then dosed from the vapor, drawn by warming a reservoir of corresponding liquid, and bled into the chamber via a precision leak valve, where its purity was monitored by mass spectrometry. The exposures quoted in Langmuirs (L) are uncorrected for the ionization gauge sensitivity.

3. Results and Discussion

3.1. X-ray Photoelectron Spectroscopy. *3.1.1. Carbon and Nitrogen (1s) XP Spectra for Multilayer Quinoline at 95 K.* Carbon (1s) and nitrogen (1s) multilayer XP spectra were acquired at 95 K following exposure of the clean Pd{111} surface to 50 L of quinoline. These are not shown and are only briefly discussed here as they were identical to the analogous spectra obtained on Pt{111} and described elsewhere.[9] The thickness of the multilayer, estimated from the attenuation of the Pd(3d) signal, was ∼20 Å.[12]

The C(1s) XP spectra showed one peak at ∼285.5 eV ± 0.5 eV with an asymmetric tail toward higher binding energy, as expected.[14−16] Analysis indicates that this latter feature contained two components at 285.2 eV ± 0.5 eV (fwhm = 1.58 eV) and 286.4 eV ± 0.5 eV (fwhm = 1.56 eV), associated with the $C_{C=C}$ (C3′ to C9′, Scheme 1) and $C_{C=N}$ (C2′ and C10′) atoms of quinoline, respectively.[9,14−16] The binding energy difference of ∼1.2 eV between these is in agreement with the energy separation reported for carbon atoms in analogous environments in other aromatic molecules of ∼1.5 eV.[15] The normalized, integrated intensities of these two carbon peaks yield a $C_{C=N}$:$C_{C=C}$ ratio of 3.5 ± 0.5, consistent with the molecular formula of quinoline, for which $C_{C=N}$:$C_{C=C}$ = 2:7.

The corresponding N(1s) XP multilayer spectrum consisted of a single peak centered at a binding energy of 399.4 eV ± 0.5 eV (fwhm = 1.29 eV), coincident with the analogous values reported for multilayers of pyridine of 399.7 eV[17] and other similar molecules.[18] After normalization by the incident beam intensity and correction for the carbon and nitrogen atomic subshell cross-sections at the relevant photon energy,[12,19] the C(1s) and N(1s) multilayer data yield a total carbon-to-nitrogen ratio, C_{total}:N_{total}, of 8.8 ± 0.9. This is in good accord with the stoichiometric ratio of 9 for C_{total}:N_{total} in molecular quinoline. Thus, the XP spectra confirm that the adsorbate retained its integrity in the multilayer formed at 95 K.

3.1.2. Carbon and Nitrogen (1s) XP Spectra for Monolayer Quinoline at 295 K. C(1s) and N(1s) XP spectra for a quinoline monolayer on Pd{111} at 295 K are shown in Figure 1, parts a and b, and are similar to those obtained for the analogous coverage on Pt{111}.[9] These spectra were acquired at incident photon energies of 430 and 530 eV, respectively, with the photon beam normal to the sample surface. The binding energy scales were calibrated against the $Pd(3d)_{5/2}$ XP peak at 335.3 eV.[20] Surface coverages were deduced from C(1s) and N(1s) XPS intensity versus exposure curves acquired at 295 K. Under these conditions, uptake ceased at the monolayer stage, thereby providing the required reference points.

The C(1s) XP spectra (Figure 1, part a) exhibit one principal feature centered at ∼285 ± 0.5 eV containing two peaks located at 284.7 ± 0.5 eV (fwhm = 1.48 eV) and 285.9 ± 0.5 eV (fwhm = 1.66 eV); that is, shifts toward lower binding energy of ∼0.5 eV in each case with respect to the corresponding emission from the multilayer. In accord with the multilayer spectra, these two peaks are assigned to the $C_{C=C}$ (C3′ to C9′, Scheme 1) and $C_{C=N}$ (C2′ and C10′) atoms of quinoline, respectively.[9,14−16] The normalized, integrated intensities yield a $C_{C=N}$:$C_{C=C}$ ratio of 3.3 ± 0.4, in reasonable agreement with the molecular

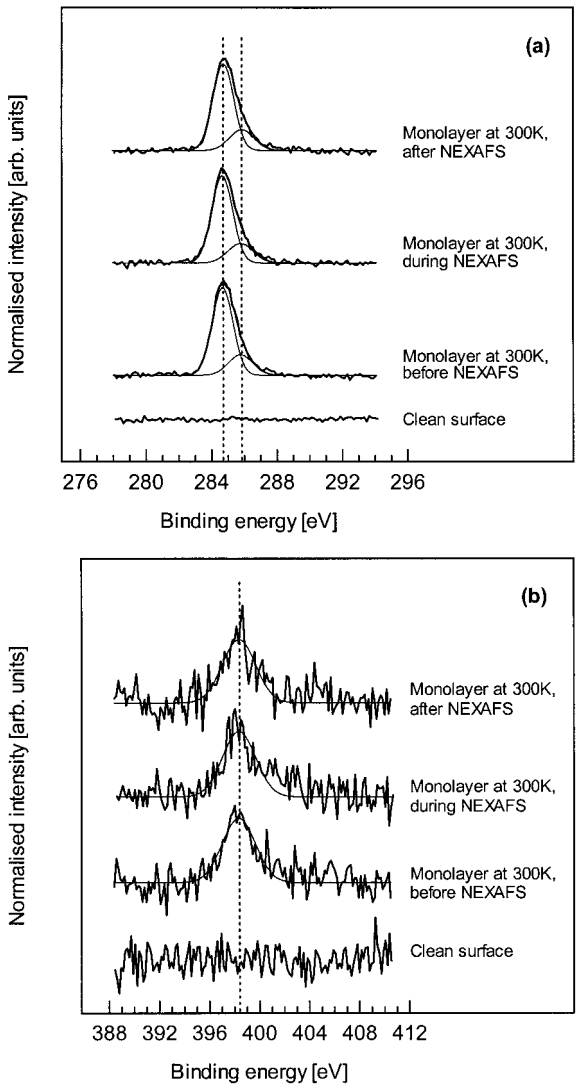

Figure 1. (a) C(1s) and (b) N(1s) XP spectra for monolayer quinoline at 295 K on Pd{111}. All spectra were recorded at photon energies of 430 and 530 eV, respectively, with the incident beam normal to the surface.

structure of quinoline, where $C_{C=N}$:$C_{C=C}$ = 2:7. Analysis of the adsorbate and substrate core level lines yields a saturation coverage at 295 K on Pd{111} of $\sim 8 \times 10^{14}$ carbon atoms·cm^{-2} ($\pm$10%), or $\sim 9 \times 10^{13}$ quinoline molecules cm^{-2} ($\pm$10%).[12] This value is consistent with the near-saturation coverages reported for similarly sized molecules on Pt{111} and Pd{111} at 295 K.[9,10,14] Analysis using the corresponding N(1s) XP intensities produced comparable values.

The N(1s) spectra exhibited one symmetrical peak centered at 398.4 $\pm$ 0.5 eV (fwhm = 2.56 eV; Figure 1, part b). As with the C(1s) monolayer spectra, it is shifted by $\sim$1.0 eV toward lower binding energy with respect to the multilayer spectrum. In both cases, these shifts to lower binding energy must reflect a combination of initial state and final state effects, which here would act in the same direction. Adsorbate $\rightarrow$ substrate charge transfer due to bond formation and increased extra-atomic relaxation around the core hole in the chemisorbed layer due to electrons in the metal would both act to decrease the measured binding energy.[12] For present purposes, the principal point is that the observed N 1s BE for the quinolone monolayer is significantly higher than that reported for atomic nitrogen ($\sim$397.3 eV) on Pd{111}[1,14,18] implying that the molecule had not undergone extensive decomposition.

These C(1s) and N(1s) binding energies for the quinoline monolayer on Pd{111} are in good agreement with those obtained in previous work for 10,11-dihydrocinchonidine (DHC)[1,10] and quinoline on Pt{111}[9] at comparable coverages (C(1s) $\sim$ 284.4 eV and N(1s) $\sim$ 398.9 eV). This indicates that the environment of the carbon and nitrogen atoms is similar for DHC and quinoline adsorbed on both Pt{111} and Pd{111}.[1,9] After correction for the carbon and nitrogen subshell cross-sections at the relevant photon energy[12,19] these XP data yield a C_{total}:N_{total} ratio of 8.4 $\pm$ 0.8, in accord with the stoichiometric ratio of 9 for C_{total}:N_{total} in quinoline. Finally, parts and b of Figure 1 indicate that the C(1s) and N(1s) XP spectra corresponding to the quinoline monolayer adsorbed on Pd{111} at 295 K do not change during the collection of the NEXAFS data, suggesting that beam-induced effects were insignificant. LEED observations (25−300 eV) showed no indication whatever, including spot-streaking, for the formation of ordered adsorbate structures.

3.2. Near edge X-ray Absorption Fine Structure Spectroscopy. *3.2.1. Multilayer Carbon and Nitrogen K-Edge NEXAFS Spectra at 95 K.* Carbon and nitrogen K-edge NEXAFS spectra for a 95 K quinoline multilayer were acquired to assist with assignment of the analogous monolayer data. Curve fitting indicated that eight resonances at 284.6 eV (A), 285.6 eV (B), 286.3 eV (C), 288.2 eV (D), 290.2 eV (E), 293.8 eV (F), 299.9 eV (G), and 305.5 eV (H) are present in the carbon K-edge spectra (Figure 2, part). Satisfactory fits were obtained when a single edge-jump was located at 290.7 eV, the value estimated for the vacuum level (VL) for this system. This value was calculated from the sum of the corresponding XPS binding energy ($\sim$285.5 eV $\pm$ 0.5 eV, section 3.1.1), which is referenced to the Fermi level, and the work function of the clean Pd{111} sample.[13] The latter was measured as 5.20 eV $\pm$ 0.05 eV for the Pd{111} crystal used here from normal emission UPS experiments. Typically, for weakly adsorbed molecules (e.g., condensed multilayers), mixing of metal and molecular states is small, and thus, the primary absorption step observed in their K-shell spectra is found to occur at or close to the vacuum level.[13] The value of 290.7 eV is also in good agreement with the corresponding ionization potentials (IP) of gas-phase benzene and naphthalene at 290.4 eV[21] and pyridine at 290.8 eV,[22] as well as with the onset of the VL continuum in the carbon K-edge NEXAFS spectra of multilayer pyridine on Pt{111}, which is located at 290.6 eV.[22]

Peaks A to E all lie below the VL (Figure 2, part a) and therefore correspond to bound state transitions. Comparison of these resonances with those in the same energy range for molecules including benzene,[22−24] pyridine,[22,25] naphthalene,[21,26] and other similar heterocyclic molecules[27,28] permits the following assignments. Peaks A and B coincide with the analogous C(1s) $\rightarrow \pi^*$(C=C) resonances in naphthalene at 284.9 eV and 285.8 eV,[21,26] respectively, and are accordingly assigned to the corresponding C(1s) $\rightarrow$ nπ^*(C=C) transitions in quinoline. Peak C at 286.3 eV is located at the energy position associated with the C(1s) $\rightarrow \pi^*$(C=N) resonances in pyrrole[28] and pyridine,[22,25] and on this basis it is assigned to the C(1s) $\rightarrow$ nπ^*(C=N) transitions in quinoline. Peak D is likely to contain contributions from both the C(1s) $\rightarrow$ nπ^*(C=C) and C(1s) $\rightarrow$ nπ^*(C=N) transitions.[22,26,28] It is also expected to include underlying intensity from C(1s) $\rightarrow \pi^*$(C−H) components which correspond to excitation processes to a mixture of Rydberg and hydrogen-derived antibonding orbitals of the same symmetry.[13,21,23]

As in naphthalene and anthracene, Peak E is located in the region containing the continuum edge-jump.[21,26,27] Additional

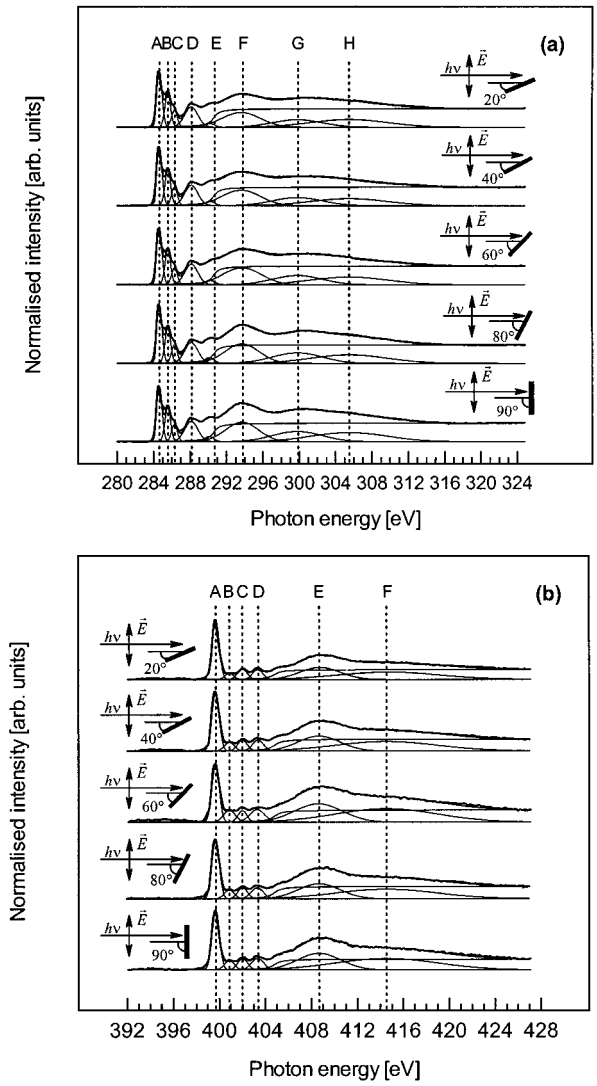

Figure 2. (a) Carbon and (b) nitrogen K-edge NEXAFS spectra for a quinoline multilayer on Pd{111} acquired at 95 K and 20°, 40°, 60°, 80°, and 90° incident photons.

intensity from *in-plane* C(1s) → σ^*(C−H) transitions is also expected in this energy range.[21,23] However, its energy position at ∼5.6 eV above Peak A coincides with that reported for C(1s) → nπ^*(C═C) transitions in both molecules and, thus, it is tentatively assigned to the analogous transitions in quinoline.

The C K-edge multilayer spectra (Figure 2, part a) exhibit three resonances that lie at 3.5 eV (F), 9.6 eV (G) and 15.2 eV (H), respectively, above the VL at 290.7 eV. These features occur widely in the NEXAFS spectra of both saturated and unsaturated molecules that contain C═C and C═N bonds.[9,23,26,28] By analogy, they are assigned to the C(1s) → σ^*(C−C) and C(1s) → σ^*(C−N); C(1s) → σ^*(C═C); and C(1s) → σ^*(C═N) resonances in quinoline, respectively. However, the highest energy continuum feature (Peak H) is very broad and weak relative to the other two, prompting argument for an alternative assignment to a multielectron "shake-up" process.[28] Here we are concerned with the analysis of the polarization dependence of the main π^* transitions in order to obtain information on the molecular orientation at the metal surface. Therefore, assignment of features F, G, and H is not critically important. Indeed, it should be emphasized that the calculation of the molecular tilt angle is not affected by the analysis of the spectra above the edge jump.[13]

The corresponding nitrogen K-edge NEXAFS spectra for the quinoline multilayer are shown in Figure 2, part b, and are similar to those obtained for quinoline multilayers on Pt{111} at the same temperature.[9] Here, as in all the NEXAFS data presented, optimized curve fits using Gaussian line shapes to model the resonances and a square step convoluted with a Gaussian line shape for the edge-jump[13] are also shown. Six resonances centered at 399.7 eV (A), 400.9 eV (B), 402.0 eV (C), 403.4 eV (D), 408.7 eV (E), and 414.5 eV (F) are discernible. The uncertainty in these energy positions is of ±0.5 eV. The most satisfactory fits were obtained when a single absorption step was fixed at 404.8 eV. This coincides with the onset of the VL continuum for multilayer pyridine on Pt{111} at 405.1 eV,[22] as well as with the IP values calculated for gas-phase quinoline at 404.5 eV[29] and pyrrole at 406.1 eV.[28]

The energy separation of Peaks B, C, and D from Peak A (1.2, 2.3, and 3.7 eV, respectively) and the ratio of the intensities of these transitions are in accord with the corresponding values predicted from theoretical calculations of the quinoline gas-phase N K-edge NEXAFS spectrum.[29] These calculations also indicate that peaks A through D belong to final states of A″-symmetry and, in a one-electron molecular orbital (MO) picture, can be understood as transitions from the N(1s) core level to the 6a″-, 7a″-, 8a″-, and 9a″-orbitals of the quinoline π-system.[29] Attribution of these features to N(1s) → nπ^* excitations is also in accord with the assignment of the analogous resonances to bound-state π^* transitions in pyridine[22] and pyrrole.[28] Above the ionization threshold, Peaks E and F correspond to the N(1s) → σ^*(C−N) and N(1s) → σ^*(C═N) shape resonances present in both pyridine and pyrrole at 408.2 eV and 413.4 eV, respectively.[22,28] The assignment of the features in the multilayer NEXAFS spectra in Figure 2, parts a and b, is summarized in Table 1. It is useful because these features are still discernible in the monolayer spectra which therefore provide a useful basis for extracting quantitative information on molecular orientation (see below). The same is not true of the corresponding carbon K-edge monolayer spectra which were broadened beyond recognition compared to the multilayer case (see below); the corresponding to theoretical calculation of the NEXAFS spectrum of the gaseous molecule were not therefore carried out.

Finally, as for benzene[24] and pyridine,[25] the main π^* resonances in the C and N K-edge NEXAFS spectra for multilayer quinoline at 95K do not demonstrate a significant polarization dependence, suggesting that the orientation of the quinoline molecules in the condensed ice is isotropic.[13] The slight variation in intensity observed may be accounted for by the polarization dependence of the contact layer that makes a nonnegligible contribution to the spectrum of the thin multilayer.[23]

3.2.2. Monolayer Carbon and Nitrogen K-Edge NEXAFS Spectra at 295 K. Carbon K-edge NEXAFS spectra for monolayer quinoline on Pd{111} at 295 K are shown in Figure 3. At all incidence angles, θ, the well-resolved π^* resonances present in the analogous multilayer spectra at 95 K (Figure 2, part a) are broadened beyond recognition and have coalesced into a single feature between ∼284 and 290 eV. A similar effect observed for monolayer quinoline[9] and benzene[22] on Pt{111} and Mo{110}[30] has been rationalized as the result of strong molecule−surface interactions. Specifically, the hybridization of molecular π-orbitals and metal d−π- orbitals and/or a reduced lifetime of the final (1s) → π^* state, due to delocalization, could account for this broadening.[13,22,30]

The near-edge absorption structure below 290 eV in Figure 3 suggests that edge-jumps corresponding to excitations from

TABLE 1: Assignment of the Carbon and Nitrogen K-Edge NEXAFS Resonances for the Quinoline Multilayer Spectra at 95K on Pd{111} Shown in Figure 2, Parts a and b

carbon K-edge NEXAFS			nitrogen K-edge NEXAFS		
resonance	energy (eV ± 0.5 eV)	assignment	resonance	energy (eV ± 0.5 eV)	assignment
A	284.6	C(1s) → π*(C=C)	A	399.7	N(1s) → π*(C=N) (6a″)
B	285.6	C(1s) → π*(C=C)	B	400.9	N(1s) → π*(C=N) (7a″)
C	286.3	C(1s) → π*(C=N)	C	402.0	N(1s) → π*(C=N) (8a″)
D	288.2	C(1s) → π*(C=C)	D	403.4	N(1s) → π*(C=N) (9a″)
		C(1s) → π*(C=N)			
		C(1s) → π*(C−H)			
E	290.2	C(1s) → π*(C=C)			
		C(1s) → σ*(C−H)			
–	290.7	edge jump		404.8	edge jump
F	293.8	C(1s) → σ*(C−C)	E	408.7	N(1s) → σ*(C−N)
		C(1s) → σ*(C−N)			
G	299.9	C(1s) → σ*(C=C)	F	414.5	N(1s) → σ*(C=N)
H	305.5	C(1s) → σ*(C=N)			

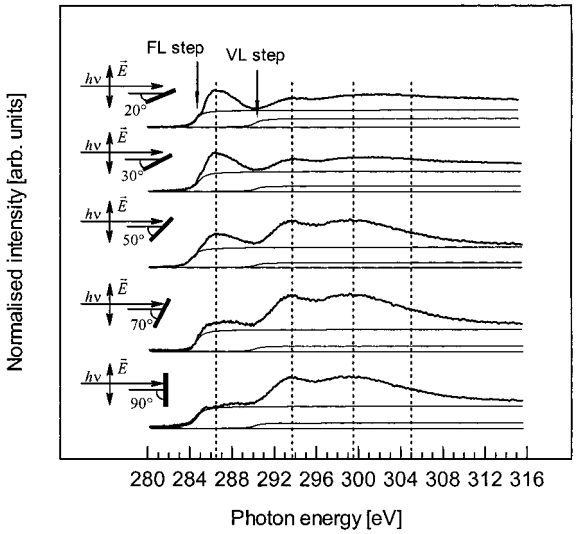

Figure 3. Carbon K-edge NEXAFS spectra for monolayer quinoline on Pd{111} acquired at 295 K and 20°, 30°, 50°, 70°, and 90° incident photons.

C(1s) core levels to both the Fermi- and vacuum-level continua are present.[13] The former is located at 284.7 eV, as expected from the C(1s) XPS binding energy (284.7 ± 0.5 eV),[13] and the latter at 290.3 eV, coincident with the VL energy of 289.9 eV, estimated from the sum of the XPS binding energy and the work function of the clean Pd{111} surface (section 3.2.1).[13] The features at 293.7 eV, 299.5 eV and 305.0 eV exhibit an opposite polarization dependence to the broad π* peak and are assigned to the C(1s) → σ*(C−C) and σ*(C−N), σ*(C=C) and σ*(C=N) transitions, respectively, as in the corresponding multilayer spectra (Figure 2, part a; Table 1).

The intensity of the broad feature containing the π* resonances is largest at grazing and smallest at normal photon incidence, consistent with an essentially flat adsorbate geometry with respect to the surface plane (Figure 3). The residual intensity at ~286.5 eV in the normal incidence spectrum not accounted for by the presence of the FL absorption step is most likely due to a minority tilted quinoline species (see below).[9,24,30] The remaining intensity between 288 eV and 290 eV at normal incidence can be attributed to (C−H)* transitions which, because they lie in the ring plane, exhibit the same polarization dependence as the higher energy σ* resonances.[13] With at least two π* features and two continuum steps, nonunique fits are likely for the region ≤290 eV in the C K-edge NEXAFS spectra for monolayer quinoline on Pd{111}at 295 K (Figure 3). Although the corresponding multilayer data are available (Figure 2, part a), in the absence of detailed indications of the energy positions and widths of the bound-state resonances, quantitative analysis of the molecular orientation of monolayer quinoline on Pd{111} at 295 K was restricted to the main π* resonance in the corresponding N K-edge NEXAFS spectra, discussed next.

The N K-edge NEXAFS spectra acquired for the 295 K quinoline monolayer shown in Figure 4, part a, resemble those for an equivalent coverage on Pt{111}.[9] Six resonances are present at 399.9 eV (A), 401.0 eV (B), 402.2 eV (C), 403.5 eV (D), 406.8 eV (E), and 413.0 eV (F). These occur at the same energies as those found for the multilayer (Table 1) and are assigned correspondingly. The shoulder on the low energy side of Peak A is present at all incidence angles and could arise from an instrumental artifact due to the non-Gaussian response of the monochromator function.[13,22] The energy separations of the π* and σ* resonances (A, B, C, and D; E and F) are very similar for the quinoline monolayers on both Pd and Pt{111}:[9] 1.4 eV, 1.2 eV, 1.3 eV, 6 eV and 1.1 eV, 1.2 eV, 1.3 eV, and 6.2 eV, respectively. Furthermore, curve fitting with parameters close to those used for the quinoline monolayer N K-edge NEXAFS spectra on Pt{111}[9] provided good fits. All the resonances present in both data sets have very similar line shapes and all exhibit the same polarization dependence: they are therefore assigned to the corresponding resonances (Table 1).

The observed broadening of the resonances for the chemisorbed overlayer (Figure 4, part a, versus Figure 2, part b) is mainly due to overlap between unoccupied metal valence band states and molecular orbitals of the adsorbate, thus shortening the lifetime of the excited state.[13] Given the similar observation for the corresponding carbon K-edge NEXAFS data (Figure 3), this provides a clear indication that the aromatic π-system plays a crucial role in the bonding of quinoline to the Pd{111} surface.[13] This inference is corroborated by the following observation. Inspection of the monolayer spectra below the vacuum level ~404 eV reveals that the finite intensity between ~401 eV and 404 eV cannot be fitted satisfactorily by an absorption step at the VL (Figure 4, part a). This discrepancy suggests the presence of another edge-jump below the VL in the monolayer spectra. Such steps are common in strongly adsorbed molecules and are located at the corresponding (1s) binding energy relative to the Fermi level (FL).[13] They result from symmetry-allowed interactions between metal and adsorbate states that are close in energy, thereby providing a continuum of final states below the corresponding VL.[13]

Satisfactory fits were obtained when a single edge jump was located at 398.5 eV, which, within the experimental uncertainty, corresponds to the N(1s) XPS binding energy relative to the Fermi level (398.4 ± 0.5 eV, section 3.1.2). As the occurrence

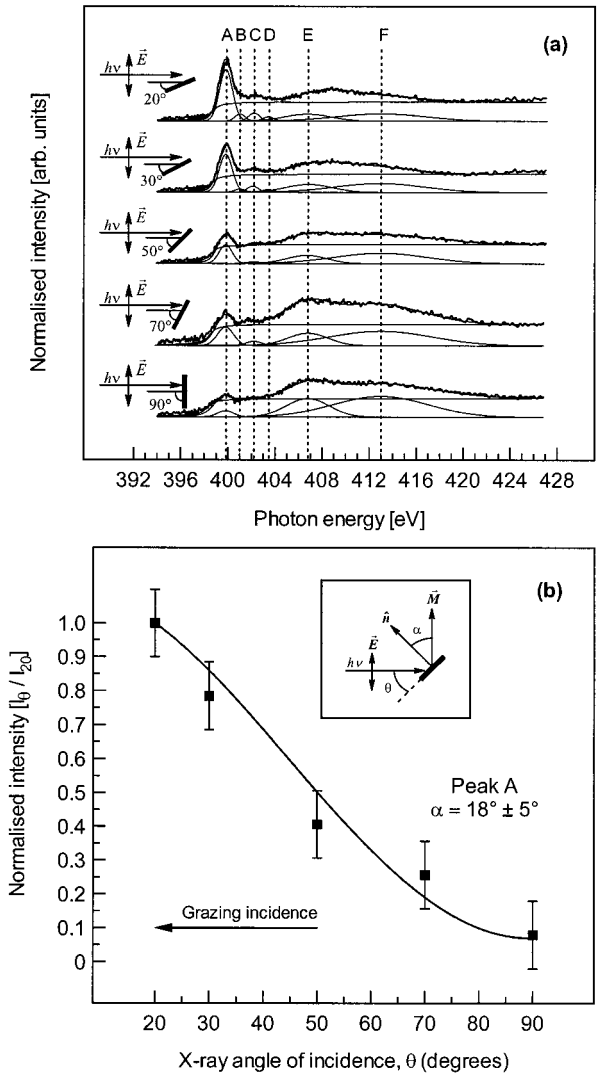

Figure 4. (a) Nitrogen K-edge NEXAFS spectra for monolayer quinoline on Pd{111} at 295 K and 20°, 30°, 50°, 70°, and 90° incident photons. (b) Plot of the normalized transition intensity for Peak A as a function of X-ray incidence angle, θ, obtained from fits of the original spectra shown in (a).

and relative size of VL and/or Fermi level steps in NEXAFS spectra depends on the nature of the chemisorption bond, the presence of a strong FL step for adsorbed quinoline is consistent with a significant π-bonding interaction with the palladium surface.[13] Furthermore, in contrast to the corresponding multilayer data (Figure 2, part b), the polarization dependence of the π^* and σ^* resonances in the monolayer spectra (Figure 4, part a) indicate *that quinoline is not randomly tilted on Pd{111}*. The first N(1s) $\rightarrow \pi^*$ transition (Peak A) represents the most reliable measure of the tilt angle of quinoline because the other π^* resonances are not sufficiently intense. Although the intensity of this feature appears greatest at grazing and virtually nil at normal photon incidence, indicative of an essentially flat-lying geometry with respect to the surface plane,[13] it does not, however, vanish completely (Figure 4, part a).

Thus, in accord with the corresponding carbon K-edge NEXAFS data (Figure 3), the angular dependence of Peak A (Figure 4, part a) is indicative of a lying-down molecular geometry. The clear interference of the FL step with the transition intensity of Peak A was accounted for by normalizing the value of the integrated intensity of this peak obtained from curve fitting by the corresponding edge-jump height in each case.[13] The molecular orientation was then determined from the variation in the π^* intensity associated with this resonance (Peak A) as a function of the photon incidence angle, θ, following standard analysis procedures.[13] The data yield a value for α, the molecular tilt angle, of 18° ± 5° with respect to the metal surface (Figure 4, part b).

Although the leading edge of the underlying absorption-step accounts for most of the intensity at $\theta = 90°$, the apparent molecular tilt angle is still relatively large. Similar behavior was found for monolayer quinoline on Pt{111} at 295K,[9] and for other supposedly "flat-lying" adsorbates such as benzene,[24,30] naphthalene,[26,27] and related systems.[23] A detailed analysis of factors that may influence such results has already been presented in the case of quinoline/Pt{111},[9] where similar results were obtained. Therefore, only a brief summary is given here.

The normalization procedure leading to the calculated tilt angle is sensitive to the π^* intensity at normal incidence so that even small extraneous contributions to the normal incidence spectra can lead to large apparent tilt angles.[13] Such contributions could arise from a strong interaction with the metal surface resulting in rehybridization, lengthening of the C−C bonds and an upward bending of the ring hydrogen atoms. The π^*-orbital would then contain some *in-plane* (σ^*) character which would be most apparent at normal incidence.[13] Alternatively, mixing of the adsorbate wave functions with those of the surface could lead to steplike backgrounds that do not necessarily follow the anticipated selection rules.[13] Neither of these possibilities seems likely here on the basis of theoretical calculations on the adsorption geometry and resulting NEXAFS spectra of quinoline on Cu{111} and Pt{111} clusters which indicate that quinoline is preferentially adsorbed on both surfaces with only very minor distortions to the planar geometry of the aromatic π-system.[29] We are therefore left with the question, does the calculated tilt angle refer to the majority species?

With pyridine[23,25] and pyrrole[31] on Pt{111} it is reasonable to suppose that the influence of the N-atom lone pair electrons could induce a significant degree of molecular tilt. However, for quinoline, such arguments do not hold because, in the absence of severe molecular distortion, the H-atom at C8′ (Scheme 1), absent in both pyridine and pyrrole, hinders the N-heteroatom from closely approaching the surface.[29,31] Thus, a majority species tilted at ∼18° seems unlikely.[25,29,31] The most reasonable explanation is that the nonvanishing intensity of Peak A at normal incidence that is not accounted for by the presence of the Fermi level step is due to the presence of a nonflat-lying minority species. Such a species might be present at step-edges or other defect sites. As even a small amount of spurious intensity at normal incidence in a π^* resonance can lead to large apparent tilt angles, the necessary concentration of such a minority state does not have to be great—∼5% of a monolayer would be sufficient—as demonstrated for benzene/Ag{110}.[24]

In summary, the carbon and nitrogen K-edge NEXAFS for monolayer quinoline on Pd{111} at 295 K indicate that this molecule is strongly bound to the surface, predominantly via the aromatic π-system. Quantitative analysis of the polarization dependence of the main π^* resonance intensity in the N K-edge NEXAFS spectra shows that quinoline is adsorbed in an essentially flat-lying configuration with a maximum tilt angle of 18° ± 5° with respect to the surface plane. This value is very close to that for quinoline on Pt{111} at 295 K (20° ± 5°).[9]

Thus it appears that the adsorption geometry of chemisorbed quinoline is essentially the same on Pt and Pd{111} at 295 K. In both cases the adsorbed layer is not randomly oriented with respect to the surface plane: an effect that could account for

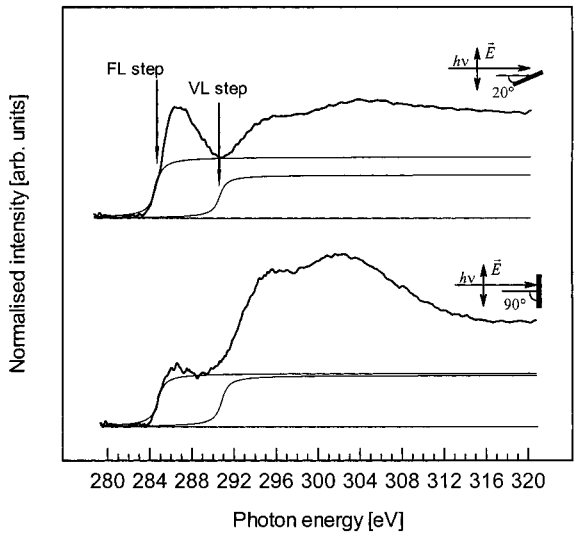

Figure 5. Carbon K-edge NEXAFS spectra for monolayer quinoline on Pd{111} acquired at 360 K for 20° and 90° incident photons.

the systematically lower rates observed with palladium catalysts. Equally, in both cases, the measured tilt angle is essentially the same and corresponds to an almost flat-lying molecule. Therefore the reversed sense of enantioselectivity observed with Pd relative to Pt is unlikely to originate from markedly different adsorption geometry in the two cases. Moreover, the combined Pd and Pt[9] results suggest that the mode of action of the chiral modifier, anchored to each surface via the quinoline moiety, is likely to be similar on both metal surfaces. Thus, our findings support the view that enantioselectivity reversal is more likely due to a change in the surface chemistry of the reactant, rather than differences in chiral modifier geometry on the two metals.

3.2.3. Monolayer Carbon K-Edge NEXAFS Spectra at 360 K. As for platinum, enantioselectivity is lost beyond ~320 K during the hydrogenation of α-ketoesters over modified palladium surfaces.[6] It has been suggested that the irreversible collapse in enantioselectivity observed beyond ~320K during the asymmetric hydrogenation of α-ketoesters may be due to a thermally induced reorientation of the anchoring moiety at the catalyst surface.[1−7,10] This would lead to a modifier adsorption geometry that is no longer compatible with that required for successful interaction with the reactant in the enantio-differentiation step, yielding a racemic mixture of products.[1−7,10]

Hence, carbon K-edge NEXAFS data were also recorded, at normal and grazing photon incidence for monolayer quinoline on Pd{111} at 360 K. The resulting spectra, shown in Figure 5, are virtually identical to those acquired for the analogous sample at 295 K (Figure 3). Two continuum jumps are present at 284.7 and 290.6 eV, and the intensity of the broad feature containing the π^* resonances, centered at ~286.5 eV, is largest at grazing and almost nil at normal photon incidence, again consistent with an essentially flat-lying adsorbate geometry.[13] Again, as at 295 K, LEED gave no indication of ordered adsorption. Therefore, as for quinoline on Pt{111}[9] the loss of enantioselectivity in the hydrogenation of α-ketoesters on modified Pd catalysts seems less likely to be due to reorientation of the chiral modifier,[1−7,10] although further experiments aimed at specifically examining this point are required. Equally, the formation or destruction of extended ordered structures as a function of temperature appears not to be an issue for both Pt and Pd. This is further evidence that the presence or absence of spatially extended arrays of chiral adsorption sites is not relevant to the appearance of enantioselective catalysis at Pd as well as Pt surfaces nor to the reversal in direction of enantioselectivity that occurs between the two metals.

The present results have another significant implication for reaction models for the heterogeneous enantioselective hydrogenation of α-ketoesters in which it is assumed that the quinoid chiral modifier anchor lies absolutely flat on the metal surface.[1−4] We have shown that for quinoline on both Pt{111}[9] and Pd{111}, this is not entirely true. Therefore, adsorption of the modifier anchor in a strictly flat-lying geometry may not be an essential requirement for effective chiral induction. Recent results for lepidine (4-methylquinoline)[9] and (*S*)-1-(1-naphthyl)-ethylamine, the parent molecule of a powerful chiral modifier, support this view.[32]

4. Conclusions

1. The orientation of chemisorbed quinoline on Pd{111} at 295 K is essentially the same as that on Pt{111}. Likewise, adsorption is disordered in both cases. The different intrinsic rates and the reversal in the sense of enantioselectivity observed for pyruvate hydrogenation on palladium catalysts relative to platinum is therefore unlikely to originate in significantly different modifier adsorption geometries or spatial distributions in the two cases.

2. At 295 K quinoline lies approximately flat on Pd{111}, strongly bound to the surface predominantly via the aromatic π-system. This adsorption geometry and the degree of long range order remain unaffected upon heating to 360 K. Thus, collapse in enantioselectivity observed around this temperature on quinoid-modified palladium catalysts seems less likely to originate from a change in the adsorption geometry of the anchoring moiety of the modifier or its spatial distribution.

Acknowledgment. Financial support from the UK EPSRC is gratefully acknowledged under grant GR/M76706. J.M.B. acknowledges the award of a CVCP Overseas Research Studentship and additional support from the Cambridge University Oppenheimer Fund and Kings' College, Cambridge.

References and Notes

(1) Simons, K. E.; Meheux, P. A.; Griffiths, S. P.; Sutherland, I. M.; Johnston, P.; Wells, P. B.; Carley, A. F.; Rajumon, M. K.; Roberts, M. W.; Ibbotson, A. *Recl. Trav. Chim. Pays-Bas* **1994**, *113*, 465.

(2) Baiker, A. *J. Mol. Catal. A: Chem.* **1997**, *115*, 473.

(3) Blaser, H. U.; Jalett, H.-P.; Müller, M.; Studer, M. *Catal. Today* **1997**, *37*, 441.

(4) Wells, P. B.; Wilkinson, A. G. *Top. Catal.* **1998**, *5*, 39.

(5) Blaser, H. U.; Jalett, H.-P.; Monti, D. M.; Reber, J. F.; Wehrli, J. T. *Stud. Surf. Sci. Catal.* **1988**, *41*, 153.

(6) Hall, T. J.; Johnston, P.; Vermeer, W. A. H.; Watson, S. R.; Wells, P. B. *Stud. Surf. Sci. Catal.* **1996**, *101*, 221.

(7) Collier, P. J.; Hall, T. J.; Iggo, J. A.; Johnston, P.; Slipszenko, J. A.; Wells, P. B.; Whyman, R. *Chem. Commun.* **1998**, 1451.

(8) Nitta, Y.; Kobiro, K. *Chem. Lett.* **1995**, 165; and *Chem. Lett.* **1996**, 897.

(9) Bonello, J. M.; Lambert, R. M. *Surf. Sci*. **2002**. In press.

(10) Evans, T.; Woodhead, A. P.; Gutiérrez-Sosa, A.; Thornton, G.; Hall, T. J.; Davis, A. A.; Young, N. A.; Wells, P. B.; Oldman, R. J.; Plashkevych, O.; Vahtras, O.; Ågren, H.; Carravetta, V. *Surf. Sci.* **1999**, *436*, L691.

(11) Wehrli, J. T.; Baiker, A.; Monti, D. M.; Blaser, H. U. *J. Mol. Catal.* **1989**, *49*, 195; *J. Mol. Catal.* **1990**, *61*, 207.

(12) Briggs C.; Seah, M. P. *Practical Surface Analysis*, 2nd ed.; Wiley-Interscience: Chichester, 1990; Vols. 1 and 2.

(13) Stöhr, J. *NEXAFS Spectroscopy*, 1st ed.; Springer: Berlin, 1996.

(14) Carley, A. F.; Rajumon, M. K.; Roberts, M. W.; Wells, P. B. *J. Chem. Soc., Faraday Trans.* **1995**, *91*, 2167.

(15) Gelius, U.; Hedén, P. F.; Hedman, J.; Lindberg, B. J.; Manne, R.; Nordberg, R.; Nordling, C.; Siegbahn, K. *Phys. Scr.* **1970**, *2*, 70.

(16) Dilks A. In *Electron Spectroscopy−Theory, Techniques and Applications*; Brundle, C. R., Baker, A. D., Eds.; Academic Press: London, 1981; p 278.

(17) Cohen, M. R.; Merrill, R. *Langmuir* **1990**, *6*, 1282; *Surf. Sci.* **1991**, *245*, 1.
(18) Nordberg, R.; Albridge, R. G.; Bergmark, T.; Ericson, U.; Hedman, J.; Nordling, C.; Siegbahn, K.; Lindberg, B. J. *Ark. Kemi* **1967**, *28*, 257.
(19) Yeh, J. J.; Lindau, I. *At. Data Nucl. Data Tables* **1982**, *32*, 1.
(20) Fuggle, J. C.; Mårtensson, N. *J. Electron Spectrosc. Relat. Phenom.* **1980**, *21*, 275.
(21) Robin, M. B.; Ishii, I.; McLaren, R.; Hitchcock, A. P. *J. Electron Spectrosc. Relat. Phenom.* **1988**, *47*, 53.
(22) Horsley, J. A.; Stöhr, J.; Hitchcock, A. P.; Newbury, D. C.; Johnson, A. L.; Sette, F. *J. Chem. Phys.* **1985**, *83*, 6099.
(23) Solomon, J. L.; Madix, R. J.; Stöhr, J. *Surf. Sci.* **1991**, *12*, 255.
(24) Liu, A. C.; Stöhr, J.; Friend, C. M.; Madix, R. J. *Surf. Sci.* **1990**, *235*, 107.
(25) Johnson, A. L.; Muetterties, E. L.; Stöhr, J.; Sette, F. *J. Phys. Chem.* **1985**, *89*, 4071.
(26) Yannoulis, P.; Dudde, R.; Frank, K.-H.; Koch, E. E. *Surf. Sci.* **1987**, *189/190*, 519.
(27) Yannoulis, P.; Frank, K.-H.; Koch, E. E. *Surf. Sci.* **1991**, *241*, 325.
(28) Newbury, D. C.; Ishii, I.; Hitchcock, A. P. *Can. J. Chem.* **1986**, *64*, 1145.
(29) Köhn, A.; Pettersson, L. G. M.; Bonello, J. M.; Lambert, R. M. In preparation.
(30) Liu A. C.; Friend, C. M. *J. Chem. Phys.* **1988**, *89*, 4396.
(31) Tourillon, G.; Raaen, S.; Skotheim, T. A.; Sagurton, M.; Garrett, R.; Williams, G. P. *Surf. Sci.* **1987**, *184*, L345.
(32) Bonello, J. M.; Williams, F. J.; Santra, A. K.; Lambert, R. M. In preparation.